GENERAL EXPERIMENTAL TECHNIQUES

MULTI-ARC PLASMA ELECTRON EMITTER FOR RADIALLY CONVERGED BEAM GENERATION

© 2025 M. S. Torba*, S. Yu. Doroshevich, M. S. Vorobyov, A. A. Grishkov, N. N. Koval, R. A. Kartavtsov, M. A. Mokeev, D.A. Shpanov

Institute of High Precision Electronics Siberian Branch

Russian Academy of Sciences, Russia, Tomsk

**e-mail: torba@opee.hcei.tsc.ru*

Received July 01, 2024

Revised August 09, 2024

Accepted October 07, 2024

Abstract. The results of studies on the generation of a radially converged electron beam in a source with a multi-arc grating plasma emitter are presented. Electron beam generation modes sufficient for surface modification of metallic materials and cylindrical products with a calculated beam energy density at the collector of up to 20 J/cm2 at pulse durations up to 500 μs have been achieved. Using an automated plasma parameter measurement system and a single Langmuir probe in the arc discharge current range of 50–120 A and a pulse duration of 50–500 μs, measurements of the distribution of the emission plasma parameters in the grid plasma emitter in the azimuthal and axial directions were carried out. Comparisons of the electronic branches of the probe characteristic at different working gas pressures (p = 5·10-2 Pa and p = 8.5·10-2 Pa) are given. The created electron source opens new opportunities for surface modification of various materials and products of cylindrical or more complex shapes with the aim of changing the functional and operational properties of this surface.

DOI: 10.31857/S00328162250125e8

1. INTRODUCTION

Plasma cathode electron sources [1–8] based on low-pressure arc discharge with grid/layer stabilization of the emission plasma boundary have repeatedly demonstrated their effectiveness in modifying the surface of various materials and products, leading to multiple improvements in the functional properties of their surfaces [9–13]. Despite the structural and technical simplicity of using planar electron beams [14–17] for processing materials and products of complex shapes, under normal conditions it is not possible to process such products with sufficient quality. Also, an undoubted disadvantage of such beams when processing products of complex shapes is the geometric shadow

effect, which does not allow for the treatment of certain areas of products with developed surfaces (for example, coronary stents).

The solution to the problems presented above is possible by generating a radially converging electron beam. However, for tasks of modifying the surface of metal products with an electron beam with a duration of tens or even hundreds of microseconds, a beam energy density of about 10 J/cm ^{2} is required, which under ballistic beam focusing conditions leads to the need to provide an emission current level of 0.15 A/cm ^{2} with an emission area of about 100 cm ^{2} and above, which is difficult to implement in sources based on thermionic and ion-electron emission.

In works [18, 19], electron beam generation is based on explosive electron emission. The electron beam in such systems is generated in a diode-type gun with an explosive emission cathode with an internal diameter of 8 cm, which incorporates 18 resistively decoupled arc plasma sources (in each cathode section) [18], as well as in a cylindrical triode-type source with a cathode diameter of 15 cm and a length of 95 cm [19]. The listed systems generate radially converging electron beams with a maximum energy density of up to 30 J/cm ^{2} at various anode diameters. However, sources based on explosive electron emission also have a number of features, namely: short pulse duration (no more than a few microseconds), relatively low cathode lifetime, beam uniformity directly dependent on the occurrence of emission centers on the cathode, difficulty in controlling beam power during its generation pulse, etc.

High energy density of the electron beam can also be provided by a plasma cathode [20], which, when stabilizing the emission plasma boundary, has several advantages over sources based on explosive electron emission, such as long service life, non-criticality to vacuum conditions, high energy efficiency. Also, by using an emission grid, it is possible to separate the discharge and accelerating gaps, which allows independent control of the main beam parameters (current, energy of accelerated electrons, pulse duration and repetition rate).

During the burning of a low-pressure arc discharge, it becomes constricted. This leads to the appearance of inhomogeneity in the emission plasma, the distribution of which in the volume of the plasma emitter affects the distribution of the beam current density. In this regard, the work is devoted to measuring the parameters of the emission plasma (concentration, electron temperature, plasma potential), determining the axial and azimuthal distributions of plasma concentration in the created multi-arc plasma emitter and demonstrating the capabilities of such an electron source for solving problems related to electron-beam modification of the surface of various materials and products.

2. METHODS AND MATERIALS

The object of study is an electron source with a grid plasma emitter *9* based on a low-pressure arc, which allows generating a radially converging electron beam (Fig. 1) with energy up to 50 keV and current up to 120 A, with pulse duration up to 500 μs and repetition rate of 1 Hz [21]. In the vacuum chamber *10* there is a multi-arc grid plasma emitter, which is a stainless steel cylinder with a length of 320 mm and an inner diameter of 220 mm, the housing of which serves as the anode of the arc discharge. The design of the plasma emitter has two main areas: area *1* , where arc discharge generation and emission plasma production occur, and area *2* , where charged particles acquire high energy corresponding to the accelerating voltage U_0 . The gaps are separated by a fine-structured metal grid *3* with a cell size of 0.14×0.14 mm^2 . Inside the plasma emitter, there is a hollow anode *4* made of stainless steel foil, which is connected through a resistor ($R_{HA} = 25$ Ohm) to the main anode. The cathode units that create the arc discharge plasma (hereinafter referred to as plasma generators) are fixed at the ends of the cylinder and spaced at an angle of 120° relative to each other, with three on each side. The working gas argon is supplied to the system through tubes of the same length, which are connected to the cathodes having an axial hole of 1 mm.

The low-pressure arc discharge is initiated by a source U_{trig} through breakdown along the surface of the dielectric *8* between the igniting electrode *5* and the cathode *6* , after which the main discharge U_d ignites in the space of the hollow anode. The hollow anode, connected through a resistor to the emission grid, allows accelerating the switching of the arc discharge current from each plasma generator to the emission grid area to increase the electron extraction coefficient from the emitter.

Extraction of electrons from the emission plasma and their acceleration to the collector *7* , which is a stainless steel rod with a diameter of 16 mm, is carried out through the cells of the emission grid under the action of a constant accelerating voltage of up to 50 kV applied between the emission electrode and the collector. The collector is located equidistant from the emitter on the axis of the electron source at a distance of 9.4 cm from the emission grid to the edge of the rod. The system parameters (discharge current I_d , collector current I_{col} , accelerating gap current I_0 and chamber current I_{ch}) are measured by Rogowski coils with a sensitivity of 50 A/V.

For all types of electron sources with a plasma cathode and grid/layer stabilization of the emission plasma boundary, important parameters responsible for stable and efficient electron beam generation are plasma concentration, its potential, and electron temperature. In this work, the measurement of arc discharge plasma parameters and probe characteristics was carried out using an automated measurement system [22]. This system allows not only to ensure the required statistical

reliability of the obtained data but also to measure plasma parameters at different moments of discharge generation and observe their dynamics. The measurement system records instantaneous values of both the probe current and the bias voltage on it. A single cylindrical Langmuir probe with a length of 5 mm and a diameter of 0.3 mm was used as the probe. The probe was located in the center of the discharge burning area equidistant from the end walls of the emitter.

The structural diagram of the measurement system is presented in Fig. 2, it consists of three blocks: the measuring block, microcontroller, and sync pulse generator. The measuring block includes an analog-to-digital converter (ADC), a voltage divider for measuring the bias voltage, and a shunt for measuring the probe current.

When generating a discharge, there is a need to synchronize the beginning of the measurement moment relative to the discharge current pulses, therefore, a synchronizing pulse generator acts as a separate unit. The maximum number of points stored in memory for a single measurement is 1000. If the number of measurements exceeds 1000, the system transfers the data to a PC and again takes measurements until it reaches the specified number of measurements. After transferring the data to the PC, the measured probe characteristic is displayed in the program window. There is also a function to change the measurement delay time from the discharge current pulse front, which allows measuring the emission plasma parameters during the discharge current pulse and tracking the dynamics of its parameters. For one generation pulse, the system measures one point of the probe I-V characteristic. Since in this case we are considering discharge generation with a frequency of 1 Hz, measuring several hundred points takes several minutes, taking into account the time for data transfer and displaying them on the screen.

The circuit for measuring probe characteristics is shown in Fig. 3. The probe was connected relative to the hollow anode of the arc discharge, which has a much larger area compared to the cathode, to introduce minimal distortions into the generated plasma. Measurement of plasma parameters (plasma potential, temperature, and electron concentration) was carried out using the electronic branch of the probe characteristic. The bias voltage was applied to the probe from a laboratory autotransformer through an isolation transformer and a diode bridge. The power supply of the measurement system was galvanically isolated from the common voltage network. The bias voltage and probe current were measured relative to the common point of the measurement system. To determine the plasma potential and electron temperature, a plot of the logarithm of the probe current versus the bias voltage was constructed. The electron saturation current was determined from the probe characteristic at the plasma potential point.

3. EXPERIMENTAL RESULTS

The arc discharge combustion voltage was measured using a high-voltage probe. Based on the obtained data, the volt-ampere characteristics (VAC) at different working gas pressures were constructed (Fig. 4). When the working gas pressure is increased, there is a decrease in the discharge combustion voltage, associated with an increase in the number of ionization acts in the volume and an increase in the concentration of the emission plasma. By way of example, at a discharge current of Id = 140 A, the discharge voltage as the gas pressure increases (from p = 2·10-2 Pa to p = 8·10-2 Pa) decreases by about 15 V.

Fig. 5 presents the results of probe measurements. From Fig. 5a, it can be seen that the plasma parameters weakly depend on pressure in the range of 50-85 mPa, whereas Fig. 5b shows a clear increase in plasma concentration with changes in discharge current. Comparison of probe characteristics obtained at different time points relative to the beginning of the pulse (Fig. 5c) showed that the plasma potential increases to approximately 60 μs and practically does not change afterward, which is probably related to the time it takes for plasma to fill the emitter volume. Also, from the probe characteristics (Fig. 5c), the plasma concentration was calculated at different time points: at the beginning of the pulse (20 μs) it was $2.6 \cdot 10^{10}$ cm^{-3}, in the middle of the pulse (60 μs) – $5 \cdot 10^{10}$ cm^{-3}, and at the end (100 μs) it reached a value of $5.8 \cdot 10^{10}$ cm^{-3}. The plasma potential during the pulse changed from 100 to 120 V. These changes indicate plasma expansion during the pulse and the establishment of a quasi-stationary generation mode by approximately the 60th microsecond.

In these experiments, the electronic saturation current varies within the range of 23-65 mA. Thus, in conditions close to operating modes, the electron temperature of the arc discharge was T_e = 35 eV, and the electron concentration in the plasma reached a value of $n_e = 8.1 \cdot 10^{10}$ cm^{-3} at a current of $I_d = 120$ A, while at a discharge current of $I_d = 80$ A the plasma concentration was $5.8 \cdot 10^{10}$ cm^{-3}, which indicates a significant dependence of concentration on the arc discharge current. It should be noted that the obtained value of T_e represents an average value of electron energy, not the energy of fully thermalized discharge electrons.

On the azimuthal distribution (Fig. 6), the plasma concentration was $n_e = (5.7 \pm 0.4) \cdot 10^{10}$ cm^{-3} at a discharge current of $I_d = 120$ A and $n_e = (3.6 \pm 0.2) \cdot 10^{10}$ cm^{-3} at a current of $I_d = 90$ A. The electron temperature averaged 40 eV, and the plasma potential was about 90 V. The obtained distribution showed satisfactory inhomogeneity of plasma concentration in this configuration of the electrode system of the plasma emitter for obtaining a uniform radially converging electron beam.

The axial distribution (Fig. 7) of emission plasma concentration along the length of the plasma emitter showed that the concentration of arc discharge plasma decreases from $9 \cdot 10^{10}$ cm^{-3} to $3 \cdot 10^{10}$ cm^{-3} as the distance from the plasma generator, on the axis of which the probe was located, increases. Probably, the obtained decrease in concentration is associated with the non-optimal radius of the circle (22 cm) on which the plasma generators are located. The plasma potential in the axial distribution changed insignificantly and was approximately 110 V.

Experiments on the generation of a radially converging electron beam using the created grid plasma emitter have shown that in this system configuration, it is possible to obtain an energy density of up to 20 J/cm^2, which is sufficient for surface treatment of metal products of various shapes. Characteristic oscillograms of the discharge current and beam current are presented in Fig. 8a. From the assumption that the entire current in the accelerating gap I_0 is the emission current from the plasma emitter $I_0 = I_{em}$, it follows (Fig. 8a) that the electron extraction coefficient from the plasma emitter, equal to the ratio $\alpha = I_{em}/I_d$, is about 0.75. Fig. 8b shows the autograph of the electron beam on a stainless steel collector at a beam current $I_b = 100$ A, accelerating voltage $U_0 = 45$ kV and pulse duration $\tau = 150$ μs ($J \approx 13$ J/cm^2).

4. CONCLUSION

The conducted studies demonstrated satisfactory plasma concentration heterogeneity filling the plasma emitter volume at various multi-arc discharge currents and working gas pressures, which indirectly may indicate uniform processing of various materials and products of cylindrical and more complex shapes using an electron source with a radially converging beam. For the azimuthal distribution in the middle of the plasma emitter, the average plasma concentration was $n_e \approx (3.6 \pm 0.2) \cdot 10^{10}$ cm^{-3} for a discharge current of 90 A and $n_e \approx (5.7 \pm 0.4) \cdot 10^{10}$ cm^{-3} for a current of 120 A. The obtained dependencies of plasma parameters on pressure showed minor differences, while when changing the discharge current from 50 to 120 A, the emission plasma concentration varied from $(3.8 \pm 0.2) \cdot 10^{10}$ cm^{-3} to $(8.1 \pm 0.2) \cdot 10^{10}$ cm^{-3}. The automated measurement system used allowed obtaining the dynamics of plasma parameters during the discharge current pulse. Thus, in the central region of the emitter, plasma is generated within 60 μs. This implies the generation of an arc discharge with a duration of about 100 μs or more in this electrode system configuration, which is also important to consider when developing electron sources based on grid plasma cathodes.

FUNDING

This work was supported by the Russian Science Foundation (project No. 23-29-00939).

REFERENCES

1. *Bugaev S.P., Kreindel Yu.E., Shchanin P.M.* Large Cross-section Electron Beams. Moscow: Energoatomizdat, 1984.

2. *Gavrilov N.V., Gushenets V.I., Koval N.N., Oks E.M. et al*. Charged Particle Sources with Plasma Emitter. Ekaterinburg: Nauka, 1993.

3. *Koval N.N., Oks E.M., Protasov Yu.S., Semashko N.N.* Emission Electronics. Moscow: Bauman Moscow State Technical University Publishing House, 2009.

4. *Kreindel Yu.E., Martens V.Ya., Sedin V.Ya., Gavrintsev S.V.* // PTE. 1982. No. 4. P. 178.

5. Efremov A.M., Kovalchuk B.M., Kreindel Yu.E., Tolkachev V.S., Shchanin P.M. *Fremov A.M., Kovalchuk B.M., Kreindel Yu.E., Tolkachev V.S., Shchanin P.M.*
// PTE. 1987. No. 1. P. 167.

6. Electron Sources with Plasma Emitter / Ed. by Yu. E. Kreindel. Novosibirsk: Nauka, 1983.

7. *Grigoriev S.V., Koval N.N., Devjatkov V.N., Teresov A.D.* // Proc. 9th Intern. Conf. on Modification of Materials with Particle Beams and Plasma Flows. Tomsk, 2008. P.19.

8. *Grigoriev S.V., Devyatkov V.N., Mikov A.V., Moskvin P.V., Teresov A.D.* // Russian Physics Journal. 2014. Vol. 57. № 11/3. P. 58.

9. *Ivanov Yu.F., Koval N.N.* Structure and Properties of Promising Metal Materials / Ed. by A.I. Potekaev Tomsk: NTL Publishing House, 2007.

10. *Grishunin V.A., Gromov V.E., Ivanov Yu.F., Denisova Yu.A.* Electron-Beam Modification of Structure and Properties of Steel. Novokuznetsk: Poligrafist, 2012.

11. *Volkov K.V., Gromov V.E., Ivanov Yu.F., Grishunin V.A.* Improvement of Fatigue Endurance of Rail Steel by Electron-Beam Treatment. Novokuznetsk: Inter-Kuzbass Publishing, 2013.

12. *Raikov S.V., Budovskikh E.A., Gromov V.E., Ivanov Yu.F., Vashchuk E.S.* Formation of Structural-Phase States and Surface Properties of Titanium Alloys during Electroexplosive Alloying and Subsequent Electron-Beam Treatment. Novokuznetsk: Inter-Kuzbass Publishing, 2014.

13. *Ivanov Yu.F., Gromov V.E., Konovalov S.V., Aksenova K.V.* Fatigue of Silumin Modified by Electron-Beam Treatment. Novokuznetsk: Poligrafist Publishing, 2016.

14. Evolution of the Surface Layer Structure of Steel Subjected to Electron-Ion-Plasma Treatment Methods / Ed. by N.N. Koval, Yu.F. Ivanov. Tomsk: NTL Publishing, 2016.

15. *Vorobyev M.S., Grigoriev S.V., Moskvin P.V., Sulakshin S.A.* // Russian Physics Journal. 2014. Vol. 57. № 11/3. P. 199.

16. *Vorobyev M.S., Gamermeister S.A., Devyatkov V.N., Koval N.N., Sulakshin S.A., Shchanin P.M.* // Technical Physics Letters. 2014. Vol. 40. № 12. P. 24.

17. *Vorobyev M.S., Devyatkov V.N., Koval N.N., Sulakshin S.A.* // Russian Physics Journal. 2017. Vol. 60. № 8. P. 109.

18. *Kiziridi P.P., Ozur G.E.* // Instruments and Experimental Techniques. 2023. № 4. P. 84. https://doi.org/10.31857/S0032816223030072

19. *Engelko V.I., Pavlov E.P., Tkachenko K.I., Shchegolikhin N.P.* // Nuclear Reactor Constants. 2019. № 1. P. 67. https://doi.org/10.55176/2414-1038-2019-1-67-74.

20. *Koval N.N., Devyatkov V.N., Vorobyev M.S.* // Izv. VUZov. Fizika. 2020. V. 63. № 12. P. 7. https://doi.org/ 10.17223/00213411/63/10/7.

21. *Torba, M.S., Doroshkevich, S.Y., Vorobyov, M.S. et al.* // Bull. Russ. Acad. Sci. Phys. 2023. № 87. Suppl. 2. P. 318. https://doi.org/10.1134/S1062873823704798

22. *Doroshkevich S.Y., Vorobyov M.S., Kovalsky S.S. et al* . // J. Physics: Conference Series. Proc. 14th Inter. Conf. "Gas Discharge Plasmas and Their Applications". 2019. V. 1393. P. 012006. https://doi.org/10.1088/1742-6596/1393/1/012006

FIGURE CAPTIONS

Fig. 1. Experimental setup diagram: *1* – arc discharge burning region, *2* – accelerating gap, *3* – fine-structured emission grid, *4* – hollow anode, *5* – ignition electrode, *6* – cathode, *7* – collector, *8* – dielectric, *9* – plasma emitter, *10* – vacuum chamber.

Fig. 2. Block diagram of the probe system for measuring emission plasma parameters.

Fig. 3. Scheme for measuring probe characteristic relative to the arc discharge anode.

Fig. 4. Current-voltage characteristic of low-pressure arc discharge in an electron source with a plasma cathode.

Fig. 5. Comparison of probe characteristics at different pressures (I_d = 70 A) (**a**), discharge currents ($p = 5 \cdot 10^{-2}$ Pa) (**b**), time moments relative to the pulse beginning (I_d = 80 A, $p = 5 \cdot 10^{-2}$ Pa) (**c**).

Fig. 6. Azimuthal distribution of emission plasma concentration ($p = 5 \cdot 10^{-2}$ Pa).

Fig. 7. Axial distribution of emission plasma concentration along the plasma generator axis ($p = 5 \cdot 10^{-2}$ Pa).

Fig. 8. Oscillograms of discharge currents and currents in the accelerating gap ($p = 5 \cdot 10^{-2}$ Pa) (**a**) and autograph of the electron beam on a stainless steel collector at beam current I_b = 100 A, accelerating voltage U_0 = 45 kV and pulse duration τ = 150 μs ($J \approx 13$ J/cm^2) (**b**).

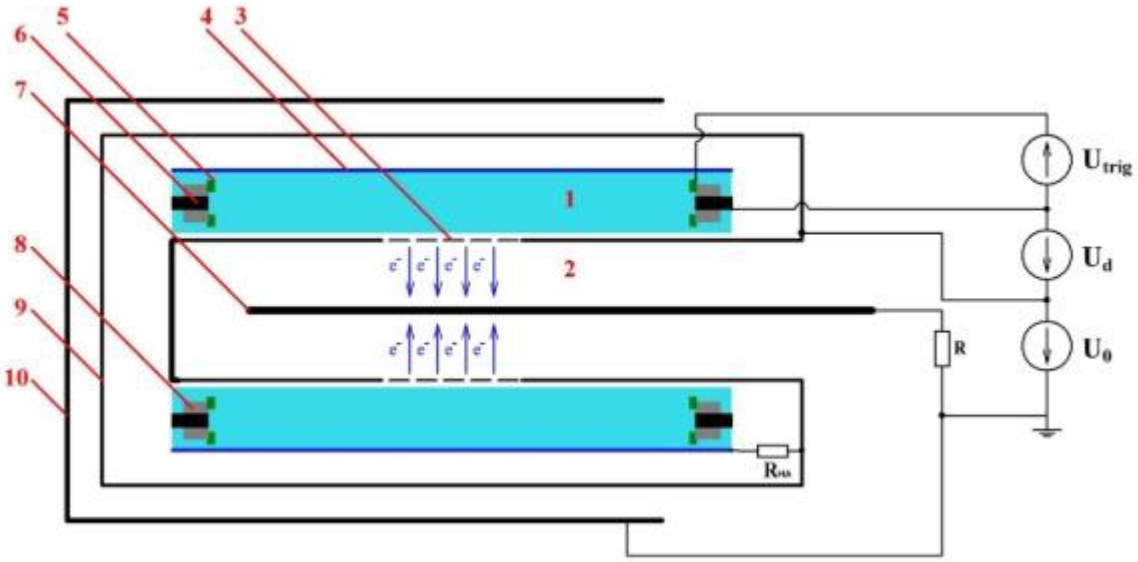

Fig. 1.

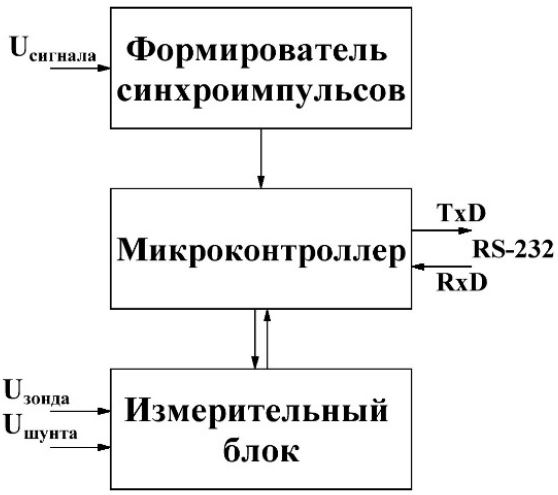
Uсигнала
Формирователь синхроимпульсов
Микроконтроллер
TxD
RS-232
RxD
Uзонда
Uшунта
Измерительный блок

Fig. 2.

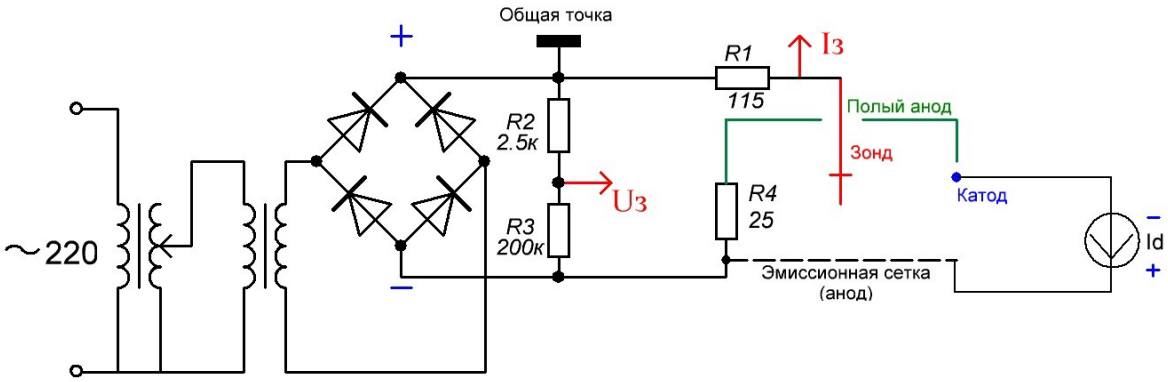
Общая точка
+
R1
115
Iз
Полый анод
Зонд
R2
2.5к
Uз
R3
200к
R4
25
Катод
~220
–
Id
+
Эмиссионная сетка
(анод)

Fig. 3.

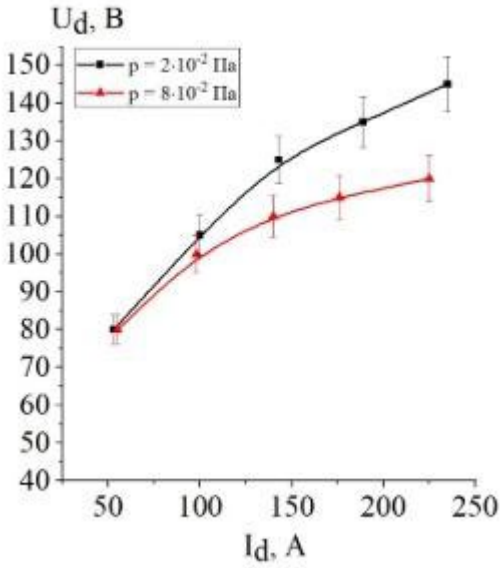
U_d, B
p = 2·10^{-2} Па
p = 8·10^{-2} Па
150
140
130
120
110
100
90
80
70
60
50
40
50
100
150
200
250
I_d, A

Fig. 4.

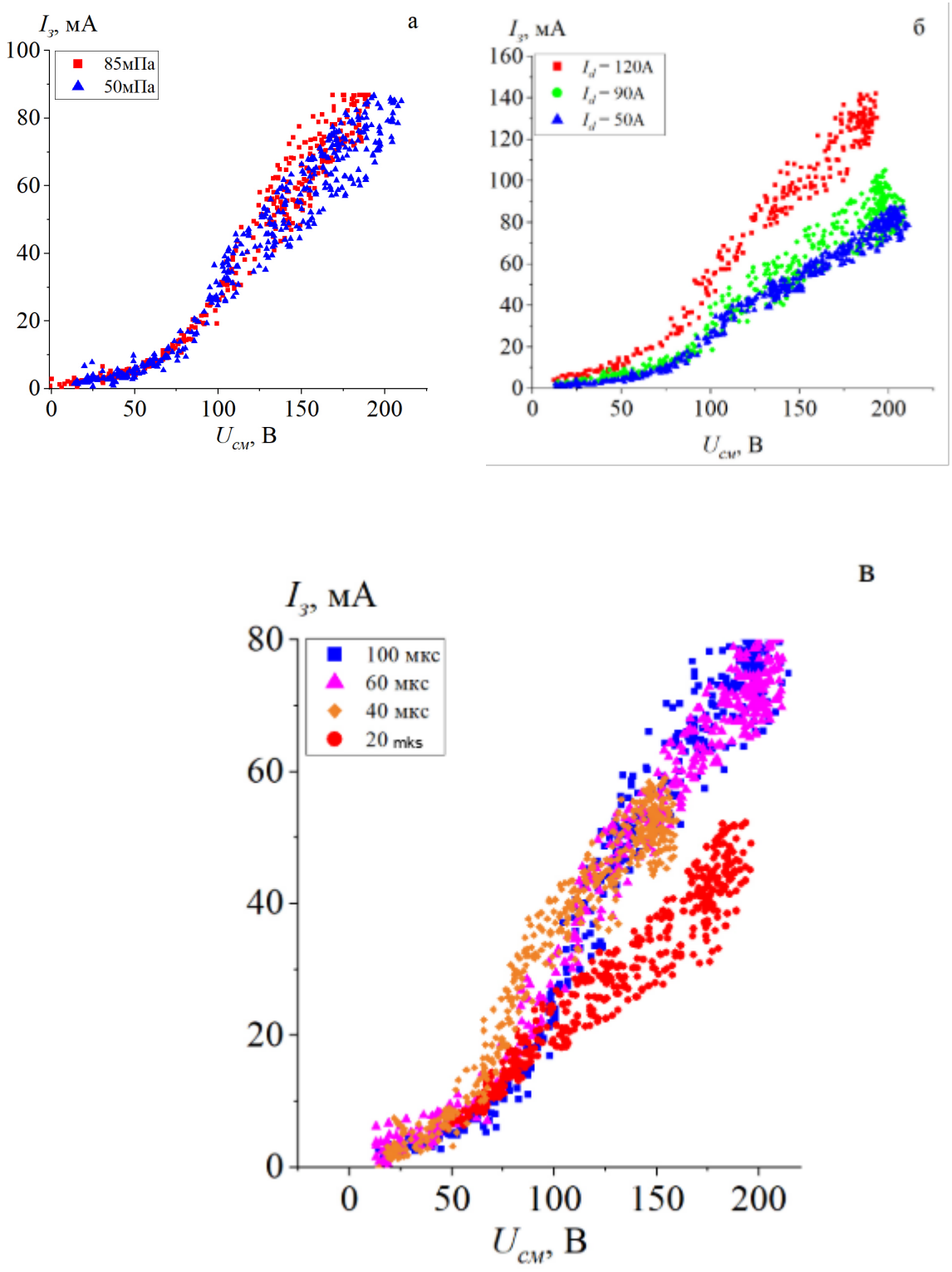
а
$I_з$, мА
85мПа
50мПа
$U_{см}$, В
б
$I_з$, мА
I_d – 120А
I_d – 90А
I_d – 50А
$U_{см}$, В
в
$I_з$, мА
100 мкс
60 мкс
40 мкс
20 mks
$U_{см}$, В

Fig. 5.

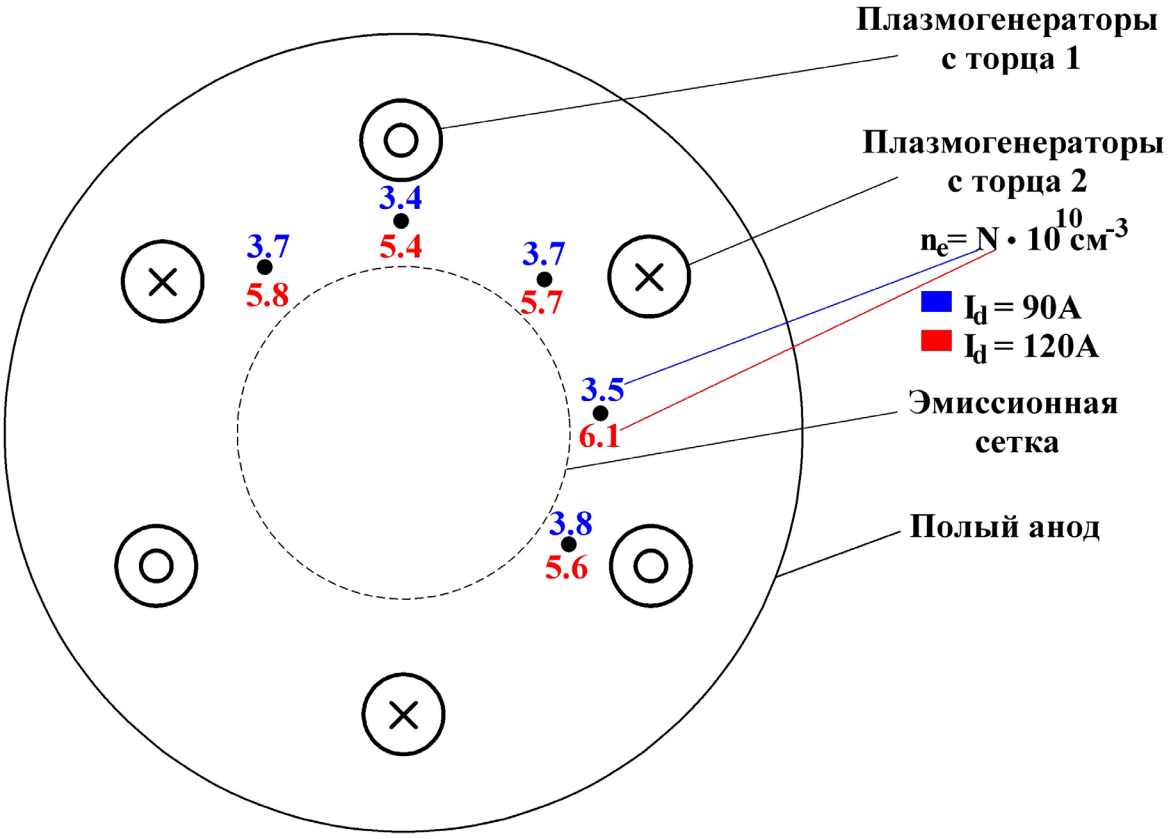
Плазмогенераторы
с торца 1
Плазмогенераторы
с торца 2
$n_e = N \cdot 10^{10}$ см$^{-3}$
I_d = 90A
I_d = 120A
Эмиссионная
сетка
Полый анод
3.4
5.4
3.7
5.8
3.7
5.7
3.5
6.1
3.8
5.6

Fig. 6.

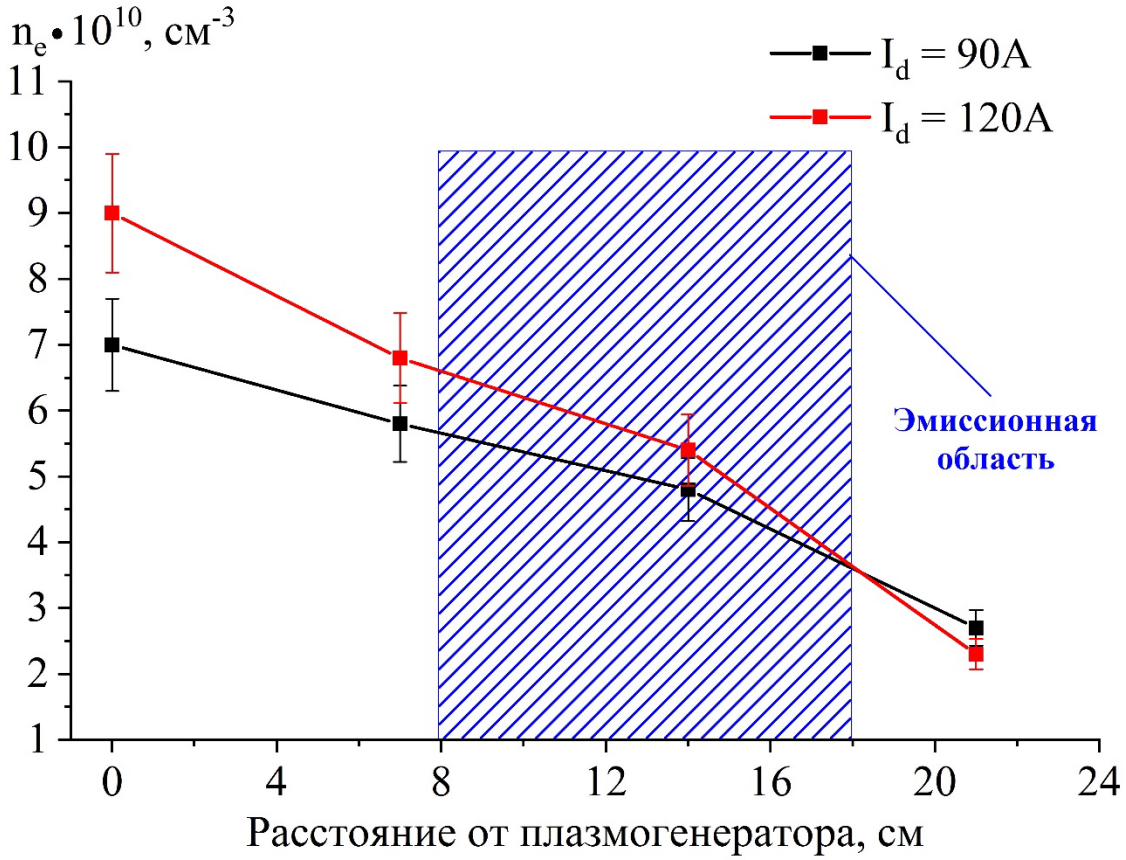
$n_e \cdot 10^{10}$, см$^{-3}$
I_d = 90A
I_d = 120A
Эмиссионная область
11
10
9
8
7
6
5
4
3
2
1
0
4
8
12
16
20
24
Расстояние от плазмогенератора, см

Fig. 7.

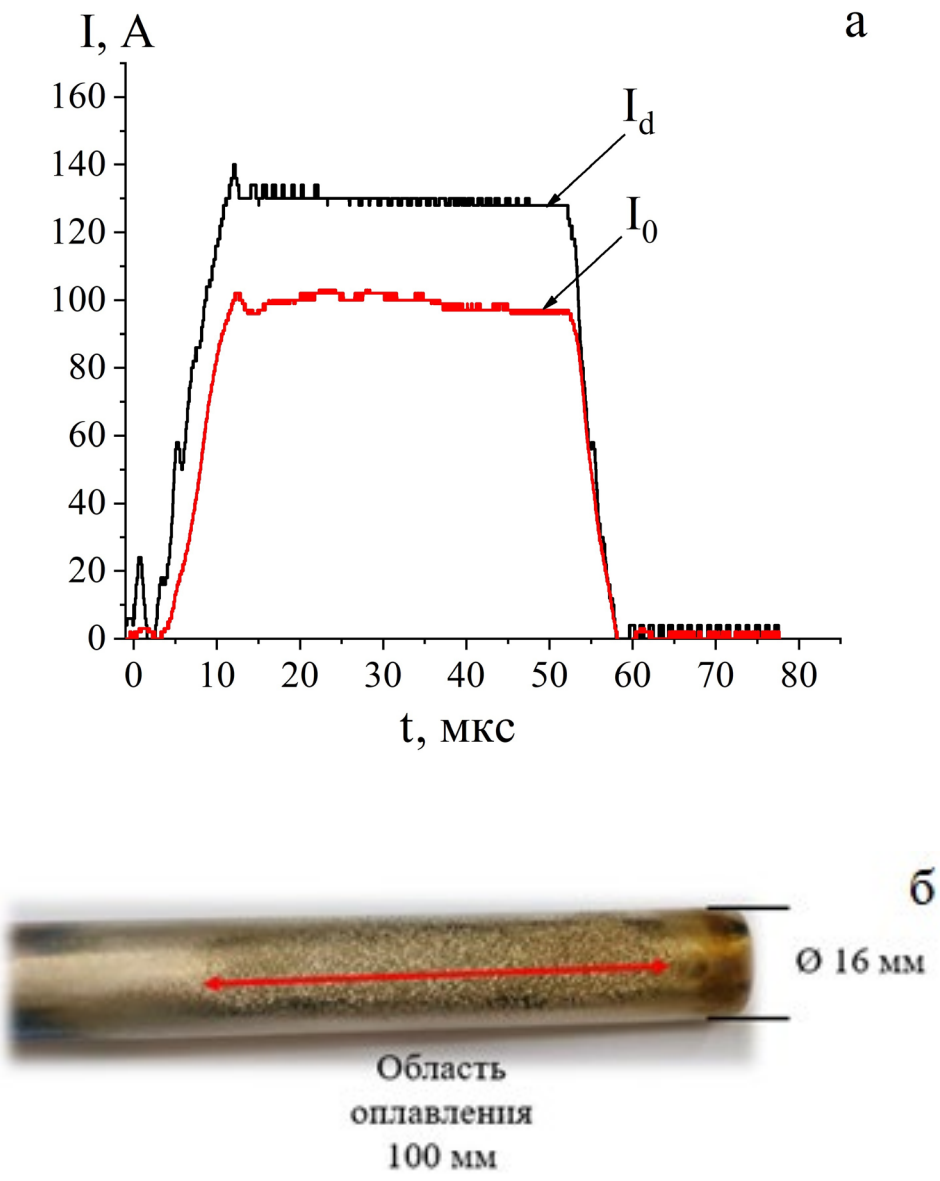
I, A
a
160
140
120
100
80
60
40
20
0
I_d
I_0
0
10
20
30
40
50
60
70
80
t, мкс
б
Ø 16 мм
Область
оплавления
100 мм

Fig. 8.